3-D Coincident Imaging Spectroscopy for Ions and Electrons

R. Dörner[1], T. Weber[1], M. Achler[1], V. Mergel[1], L. Spielberger[1], O. Jagutzki[1], F. Afaneh[1], M.H. Prior[3] C.L. Cocke [2]and H. Schmidt-Böcking[1]

[1]Institut für Kernphysik, Universität Frankfurt, August Euler Str. 6, D60486 Frankfurt, Germany
[2]Department of Physics, Kansas State University, Manhattan, KS 66506
[3]LBNL, Berkeley, CA 94720

Novel imaging techniques allow the coincident determination of the vector momenta of several ions and electrons from ionizing interactions of photons or charged particles with atoms or molecules. These devices combine 4 π solid angle with high resolution in momentum space. They deliver multidimensional images of the multi-particle breakup processes. Electrostatic and pulsed electric fields, magnetic fields and multi-hit capable micro-channel plate detectors are combined in such devices. We focus on some technical aspects and discuss an application to study single ionization in ion-atom collisions.

Introduction

The investigation of few-particle transitions in atoms or molecules induced by photons or charged particles are a fascinating test ground for our understanding of many-body dynamics in quantum mechanics. Such dynamics of Coulomb systems is the governing factor for much of the structure and evolution in our everyday world. Atomic and molecular many-particle reactions are characterized by fully differential cross sections (FDCS), i.e. cross sections differential in all observables of the final state. In an ionization process of an atom this typically corresponds to the vector momenta, spins and internal excitation of all reaction products. Such FDCS provide the most stringent test for theory. Any integration over observables often masks important characteristics of the process. In turn, experimental FDCS in the best case directly unveil mechanisms of the many-particle transition. Tremendous progress in measuring such FDCS have been made in the field of (e,2e) collisions (see [1, 2, 3] for reviews) and $(\gamma, 2e)$ experiments by detecting two electrons with traditional spectrometers in coincidence (see e.g. [4, 5, 6, 7, 8, 9, 10, 11, 12]). Coincident momentum space imaging for atomic and molecular reactions which is the subject of this article differs from coincident electron detection techniques mainly by the fact that it covers the full final state phase space of the reaction and that it can be used for the study of ion-atom collisions. Technically it also differs from most of the chemistry imaging work reported in this book by the fact that coincident single particle counting is used.

The basic principles for 3-dimensional coincident momentum space imaging are identical for ion and electron detection. They are based on a small reaction volume (typically below 1 mm^3) from which the fragments are guided by electric and magnetic fields to large area position sensitive detectors. The momenta of electron and ion can then be calculated from the time of flight and the position where the particles hit the detectors.

General considerations for momentum space imaging

The dynamic range of typical energies, momenta and particle masses which is of relevance in the different fields of application of momentum space imaging is several orders of magnitude. We list some examples:

- Slow ion-atom collisions: For reactions like

$$10keVp + He \rightarrow p + He^{1+} + e^- \tag{1}$$

  typical momenta of the electrons are below 0.6 a.u. (atomic units) corresponding to 5 eV, the momenta of the He^{1+} ions are below 20 a.u. corresponding to an ion energy of 740 meV [13].

- Fast Ion-atom collisions: For reactions like

$$1MeVp + He \rightarrow p + He^{1+} + e^- \tag{2}$$

  electrons of up to few hundred eV are of interest and ion momenta are in the range of 1 a.u. corresponding to only 1.9 meV ion energy (this holds for other projectils with similar velocity as well).

- VUV photon-atom interaction: For example

$$80eV\gamma + He \rightarrow He^{2+} + 2e^- \tag{3}$$

  results in electrons below 1 eV (higher photon energies however lead to higher electron energies) and ion momenta of about 0.2 a.u. or energies of 0.07 meV [14].

- Ionization of atoms by femtosecond lasers in the 10^{14}-10^{15} W/cm^2 regime leads to typical electron energies below 1 keV and ion momenta below 10 a.u. [15, 16].

- Ionization of molecules by ion, photon or laser impact leads to electron energies similar to the ionization of an atom but to ion energies reaching up to 10 eV.

The task is to find field configurations which guide particles with masses from the electron mass up to several 10^5 times the electron mass and energies from a few μeV up to several 100 eV towards the position sensitive detectors. The general ingredients used to achieve a projection of these very different particles are the combination of static electric and magnetic fields for the electrons and static and pulsed electric fields with lenses for the ion imaging.

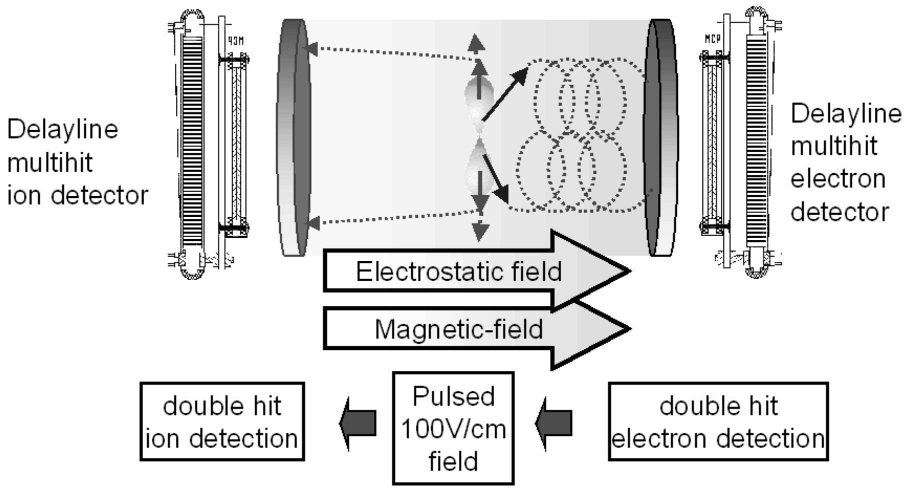

Figure 1: *Schematic of coincident momentum space imaging spectrometer for the investigation of multiple ionization of molecules. A superposition of a weak (few V/cm) electrostatic field and a magnetic field guides the electrons from the reaction volume onto a position sensitive channel plate detector with delayline readout, which is capable of decoding the position of multiple hits. After arrival of the electrons the electric field is pulsed to 80 V/cm to collect the heavy fragment of the molecule onto a second position sensitive detector. Positions and times-of-flight of all particles are recorded in event mode.*

The schematic of a spectrometer used for the investigation of double ionization of D_2 by 80 eV photons is shown in figure 1. For this application electron energies range from 0-20 eV and equal mass ions with about 9.5 eV energy each are expected. To achieve 4π solid angle for the electrons an electrostatic field of about 3V/cm and a magnetic field of 10 gauss was used. The low electrostatic field was necessary first to spread the two electrons out in time over about 100 nsec to circumvent multihit dead time of the detector and second to improve the momentum resolution in the time-of-flight direction. After the electrons reached the detector the electric field was pulsed to about 80 V/cm to collect the ionic fragments.

Momentum and spatial width of the target

A general limit for the resolution achievable is given by the internal momentum distribution in the target. At room temperature the thermal motion of helium corresponds to 4.6 a.u. of momentum, thus some cooling technique is essential. With the use of supersonic gas jet targets the momentum spread can be easily improved by about a factor of 100, giving a limit of around 0.05 a.u. or 4.6 μeV. For heavier targets this gets much worse, for two reasons. First typically the speed ratio of supersonic jets is best for helium and worse for heavier gases and the gas nozzles cannot be cooled to 30 K as it can be done for helium. Second the thermal energies stay constant, thus the momenta increase with the square root of the mass. For studies of molecular breakup this is mostly not a severe limitation, since the typical momenta are large, for ionization studies of heavier atoms this becomes a limitation. The use of laser cooled trapped atoms instead of supersonic beams [17] will yield a great improvement in resolution.

Besides the momentum spread of the target also the spatial extension of the target needs to be considered. For ion imaging 3-dimensional focussing has been effectively used to circumvent this problem. In the direction of the electric field a proper choice of acceleration and field free regions can be chosen to make the time-of-flight independent of the starting point of the trajectory [18]. In the two dimensions perpendicular to the electric field electrostatic lenses can be used to focus particle trajectories starting at different positions in the reaction volume to the same position on the detector. The field geometries must be chosen such that the focal plane of the time-of-flight focussing coincides with the focal plane of the lens. Ideally one aims for non dispersive focusing. In electrostatic lenses this requires in general that the energy of the particle when passing the lens is similar for all particles. This means that the energy acquired in the extraction field before entering the lens should by large compared to the energy from the collision. For reactions with atoms where typical ion energies are in the meV regime, this is already achieved with typical extraction field of a few V/cm. For electrons and ions from molecular breakup however very high extraction fields (several 100 V/cm) are necessary. Such high fields effect the momentum measurement in the time-of-flight direction. A field of 1 V/cm corresponds to a difference of flight time of 125nsec for singly charge particles starting with zero or 1 a.u. momentum respectively. This scales linearly with the extraction voltage. Thus fields in the range of 100 V/cm result in no or extremely bad momentum resolution in the time-of-flight direction. Therefore a combination of high resolution in the time-of-flight direction and focussing is hard to achieve for higher energetic particles.

Magnetic Guiding Fields for Electrons

Electrons with very low energy (up to a few eV) can be efficiently projected onto the detector with fields which are low enough to archive reasonable resolution in the time-of-flight direction. However, the electron detector need to be placed close (a few cm) to the interaction volume to provede a solid angle close to 4π. To guide also electrons with higher momenta transverse to the electric field Moshammer and Ullrich introduced electron imaging with a homogenous magnetic field superimposed parallel to the electric extraction field [19, 20]. The magnetic field forces the electrons into spiral trajectories and thus prevents them from leaving the spectrometer. The revolution time does not depend on the electron momentum. It scales linearly with the magnetic field. By measuring the time-of-flight and the position of impact on the detector the two momentum components perpendicular to the field can be deduced. For time-of-flights which coincide with integer multiples of the revolution time the electrons return to the projection of their starting point on the detector, independent of their momenta. For such times the information regarding the perpendicular momentum is lost.

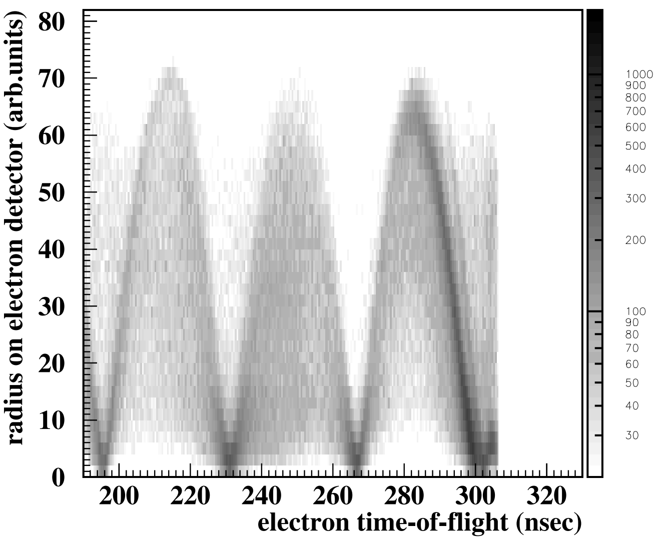

Figure 2: *Distance of electron impact from center of electron detector versus time-of-flight of the electron. The time-of-flight zero increases from right to left, zero is in channel 336. The magnetic field is about 10 gauss, the electrons are from double ionization of D_2 by 80 eV photon impact. The nodes correspond to full turns of the electrons in the magnetic field.*

Figure 2 shows the radial distance from the projected position of the reaction volume as a function of the time-of-flight of the electrons. The nodes of the distribution spaced by the revolution time are clearly seen. This gives a highly accurate online calibration of the magnetic field. A magnetic field of 10 Gauss yields a revolution time of 32 nsec. It collects electrons of up to 40 eV onto a detector of 80mm active diameter. The electron spectrometer configuration with electric and magnetic field yields a unique combination of 4π solid angle up to relatively high electron energies and high resolution in all three dimensions by effectively decoupling the transverse and longitudinal motions. A practical limit for the magnetic field strength and thus the maximum acceptable transverse momentum is given by the revolution frequency. With a typical time-of-flight resolution of 0.5 nsec at fields higher than about 30-40 Gauss (8-10- nsec revolution time) the resolution in the transverse momentum decreases strongly.

Applications to ion-atom collisions

There are already many examples for multiphoton ionization of molecules in this book. Therefore we choose single ionization in ion-atom collisions as an example to illustrate the power of coincident momentum space imaging for unveiling the driving mechanism of a few-body process. In general single ionization (as equations 1 or 2) is a three-body momentum exchange process. One can approximate it by splitting it in three separate two-body momentum exchange processes between projectile-electron, projectile-ion and electron-ion. Although all three pair-wise interactions are always present, there are paradigmatic cases where one of the three dominates. As example for the dominance of the projectile-ion momentum exchange we discuss 10 keV impact energy and as example where projectile-electron is important we show 0.5 MeV impact energy. These data have been measured by coincident imaging of the momentum vector of the electron and the recoiling ion. The momentum change of the projectile is determined for each event using momentum conservation.

Figure 3 shows the final state momenta of reaction 1, corresponding to a collision velocity of 0.63 a.u.. Thus contrary to most of the chemical 'collisions' discussed in this book here the velocity is of the same order of magnitude as the orbital velocity of the electrons. The electron is not ejected by additional laser assistance, but dynamically from the collision itself. The figure shows that only little momentum is transferred to the electron while the main momentum exchange is between the projectile and the recoiling ion. As the proton approaches the helium atom for a short time a quasi-molecule is formed in which the electron acts as 'glue' which pulls the recoiling ion in the forward direction. As this quasi-molecule breaks apart, in most of the cases the electron relaxes to a bound state of either the projectile or the target. This major channel is not shown in the figure. Only in about 10 % of the collisions is the electron promoted into a continuum state. This channel is shown in figure 3. As can be expected from the above picture of a quasi-adiabatic electron promotion, the momentum exchange between the two

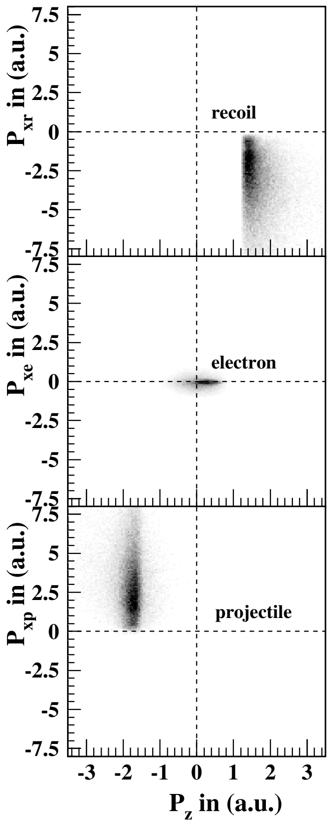

Figure 3: *Projection of the momentum transfer vectors of the* He^{1+} *recoil-ion (upper) electron (middle) and projectile (lower) in the final state onto the plane defined by the projectile beam and the momentum vector of the recoil-ion for 10* $keV/u\ p + He \rightarrow He^{1+} + e^- + p$. *The* $+p_z$ *axis is parallel to the incoming projectile direction, the* $+p_y$ *axis is parallel to the final transverse momentum component of the recoil-ion. The grey scale represents the corresponding doubly differential cross section* $d^2\sigma/(dk_x dk_\parallel)$ *on a linear scale (similar to [21]).*

nuclei is dominant, the electron is stranded with very little momentum in between the two centers.

If the projectile velocity is raised to 6.3 a.u. the momentum exchange pattern changes completely (figure 4). Here the projectile passes so fast that no quasi-molecule can be formed. Ionization becomes the main reaction channel. One of the mechanisms leading to the emission of the electron is now a binary encounter between the fast projectile and the bound electron. This can be seen in figure 4 from the partly back to back emission of projectile and electron. The recoiling ion is, contrary to figure 3 no longer pulled in the forward direction.

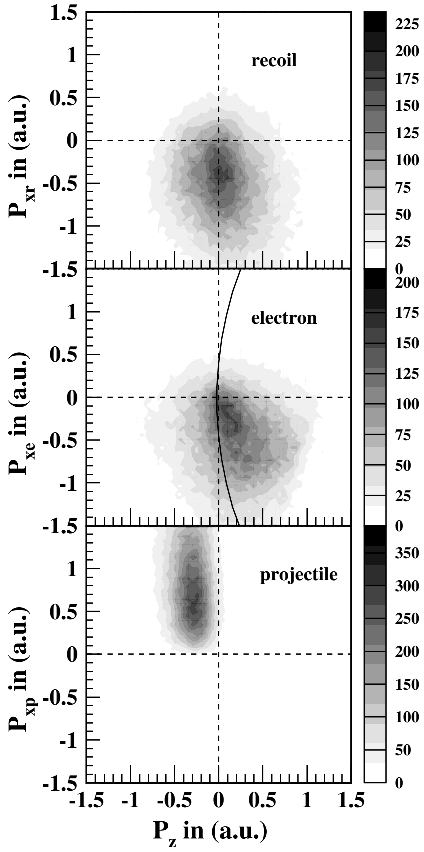

Figure 4: *0.5 MeV/u* $p + He \rightarrow He^{1+} + e^- + p$. *Projection of the momentum transfer vectors of* He^{1+} *recoil-ion (upper) electron (middle) and projectile (lower) in the final state onto the plane defined by the projectile beam and the scattered projectile. The* $+p_z$ *axis is parallel to the incoming projectile direction, the* $+p_y$ *axis point in the direction of the scattered projectile. The grey scale represents the corresponding doubly differential cross section* $d^2\sigma/(dk_x dk_\parallel)$ *on linear scale. The circular arc in the middle figure shows the location of the binary encounter ridge for electrons (from [22]).*

A great amount of coincident 3-dimensional momentum space imaging studies have been performed in the previous 10 years. They include electron impact ionization of atoms [23, 24], single photon double ionization of atoms from threshold [14, 25, 26, 27, 28, 29] to 100 keV [30, 31] and ion impact on atoms from keV protons [13] to GeV/u U^{92+} [32] projectiles, capture and transfer reactions [33, 34], multiphoton double and triple ionization by femto second laser pulses [15, 16] and single photon double ionization of fixed in space molecules [35]. An overview can be found in [36]. The unprecedented resolution and completeness of many of those investigations allowed the resolution of some long-standing puzzles in atomic collision physics but at the same time raised even more fundamental questions.

Acknowledgements

The work was financially supported by DFG, BMBF and by the Division of Chemical Sciences, Basic Energy Sciences, Office of Energy Research, U.S.Department of Energy. H.B. and R.D. acknowledge support from the Alexander von Humboldt foundation. F.A. greatfully acknowledges support by the DAAD. We also acknowledge financial support from Max Planck Forschungspreis of the Humboldt foundation. We acknowledge helpful discussion with our colleagues Y.D. Wang, S. Keller, R. Dreizler, C. Whelan, J. Walters, H. Khemliche.

References

[1] M.A. Coplan et al. *Rev.Mod.Phys.*, 66:985, 1994, and References therein.

[2] I.E. McCarthy and E. Weigold. *Rep. Prog. Phys.*, 54:789, 1991.

[3] A. Lahmam-Bennani. *J. Phys*, B24:2401, 1991.

[4] O. Schwarzkopf, B. Krässig, J. Elmiger, and V. Schmidt. *Phys. Rev. Lett.*, 70:3008, 1993.

[5] O. Schwarzkopf, B. Krässig, V. Schmidt, F. Maulbetsch, and J. Briggs. *J. Phys.*, B27:L347–50, 1994.

[6] O. Schwarzkopf and V. Schmidt. *J. Phys.*, B28:2847, 1995.

[7] A. Huetz, P. Lablanquie, L. Andric, P. Selles, and J. Mazeau. *J. Phys.*, B27:L13, 1994.

[8] G. Dawber, L. Avaldi, A.G. McConkey, H. Rojas, M.A. MacDonald, and G.C. King. *J. Phys.*, B28:L271, 1995.

[9] P. Lablanquie, J. Mazeau, L. Andric, P. Selles, and A. Huetz. *Phys. Rev. Lett.*, 74:2192, 1995.

[10] J. Viefhaus, L. Avaldi, F. Heiser, R. Hentges, O. Gessner, A. Rüdel, M. Wiedenhöft, K. Wielczek, and U. Becker. *J. Phys.*, B29:L729, 1996.

[11] J. Viefhaus, L. Avaldi, G. Snell, M. Wiedenhöft, R. Hentges, A. Rüdel, F. Schäfer, D. Menke, U. Heinzmann, A. Engelns, J. Berakdar, H. Klar, and U. Becker. *Phys. Rev. Lett.*, 77:3975, 1996.

[12] J.P. Wightman, S. Cveejanovic, and T.J. Reddish. *J. Phys.*, B31:1753, 1998.

[13] R. Dörner, H. Khemliche, M.H. Prior, C.L. Cocke, J.A. Gary, R.E. Olson, V. Mergel, J. Ullrich, and H. Schmidt-Böcking. *Phys. Rev. Lett*, 77:4520, 1996.

[14] R. Dörner, J. Feagin, C.L. Cocke, H. Bräuning, O. Jagutzki, M. Jung, E.P. Kanter, H. Khemliche, S. Kravis, V. Mergel, M.H. Prior, H. Schmidt-Böcking, L. Spielberger, J. Ullrich, M. Unverzagt, and T. Vogt. *Phys. Rev. Lett.*, 77:1024, 1996. see also erratum in Phys. Rev. Lett. 78. 2031 (1997).

[15] Th. Weber et al. *Phys. Rev. Lett*, , submitted for publication.

[16] R. Moshammer et al. *Phys. Rev. Lett*, , submitted for publication.

[17] S. Wolf and H. Helm. *Phys. Rev.*, A56:R4385, 1997. .

[18] W.C. Wiley and I.H. McLaren. *Rev. Sci. Instr.*, 26:1150, 1955. .

[19] R. Moshammer, M. Unverzagt, W. Schmitt, J. Ullrich, and H. Schmidt-Böcking. *Nucl. Instr. Meth.*, B 108:425, 1996.

[20] H.Kollmus, W. Schmitt, R. Moshammer, M. Unverzagt, and J. Ullrich. *Nucl. Instr. Meth.*, B124:377, 1987.

[21] R. Dörner, V. Mergel, L. Spielberger, M. Achler, Kh. Khayyat, T. Vogt, H. Bräuning, O. Jagutzki, T. Weber, J. Ullrich, R. Moshammer, M. Unverzagt, W. Schmitt, H. Khemliche, M.H. Prior, C.L. Cocke, J. Feagin, R.E. Olson, and H. Schmidt-Böcking. *Nucl. Instr. Meth.*, B127:225–31, 1997.

[22] Th. Weber. Master's thesis, Diploma Thesis, University Frankfurt, 1998. unpublished.

[23] O. Jagutzki, L. Spielberger, R. Dörner, s: Nüttgens, V. Mergel, H. Schmidt-Böcking, J. Ullrich, R.E. Olson, and U. Buck. *Zeitschrift für Physik*, D36:5, 1996.

[24] A. Dorn, R. Moshammer, C.D. Schröter, T. Zouros, W. Schmitt, H. Kollmus, R. Mann, and J. Ullrich. *Phys. Rev. Lett*, 82:2496, 1999.

[25] R. Dörner, T. Vogt, V. Mergel, H. Khemliche, S. Kravis, C.L. Cocke, J. Ullrich, M. Unverzagt, L. Spielberger, M. Damrau, O. Jagutzki, I. Ali, B. Weaver, K. Ullmann, C.C. Hsu, M. Jung, E.P. Kanter, B. Sonntag, M.H. Prior, E. Rotenberg, J. Denlinger, T. Warwick, S.T. Manson, and H. Schmidt-Böcking. *Phys. Rev. Lett.*, 76:2654, 1996.

[26] R. Dörner, H. Bräuning, J.M. Feagin, V. Mergel, O. Jagutzki, L. Spielberger, T. Vogt, H. Khemliche, M.H. Prior, J. Ullrich, C.L. Cocke, and H. Schmidt-Böcking. *Phys. Rev.*, A57:1074, 1998.

[27] H.P Bräuning, R. Dörner, C.L. Cocke, M.H. Prior, B. Krässig, A. Bräuning-Demian, K. Carnes, S. Dreuil, V. Mergel, P. Richard, J. Ullrich, and H. Schmidt-Böcking. *J. Phys.*, B30:L649, 1997.

[28] H.P Bräuning, R. Dörner, C.L. Cocke, M.H. Prior, B. Krässig, A. Kheifets, I. Bray, A. Bräuning-Demian, K. Carnes, S. Dreuil, V. Mergel, P. Richard, J. Ullrich, and H. Schmidt-Böcking. *J. Phys.*, B31:5149, 1998.

[29] V.Mergel, M. Achler, R. Dörner, Kh. Khayyat, T. Kambara, Y. Awaya, V. Zoran, B. Nyström, L.Spielberger, J.H. McGuire, J. Feagin, J. Berakdar, Y. Azuma, , and H. Schmidt-Böcking. *Phys. Rev. Lett.*, 80:5301, 1998.

[30] L. Spielberger, O. Jagutzki, B. Krässig, U. Meyer, Kh. Khayyat, V. Mergel, Th. Tschentscher, Th. Buslaps, H. Bräuning, R. Dörner, T. Vogt, M. Achler, J. Ullrich, D.S. Gemmel, and H. Schmidt-Böcking. *Phys. Rev. Lett.*, 76:4685, 1996.

[31] L. Spielberger, H. Bräuning, A. Muthig, J.Z. Tang, J. Wang, Y. Qui, R. Dörner, O. Jagutzki, Th. Tschentscher, V. Honkimäki, V. Mergel, M. Achler, Th. Weber, Kh. Khayyat, J. Burgdörfer, J. McGuire, and H. Schmidt-Böcking. *Phys. Rev.*, 59:371, 1999.

[32] R. Moshammer, J. Ullrich, W. Schmitt, H. Kollmus, A. Cassimi, R. Dörner, R. Dreizler, O. Jagutzki, S. Keller, H.-J. Lüdde, R. Mann, V. Mergel, R.E. Olson, T. Prinz, H.Schmidt-Böcking, and L Spielberger. *Phys. Rev. Lett*, 79:3621, 1997.

[33] V. Mergel, R. Dörner, J. Ullrich, O. Jagutzki, S. Lencinas, S. Nüttgens, L. Spielberger, M. Unverzagt, C.L. Cocke, R.E. Olson, M. Schulz, U. Buck, E. Zanger, W. Theisinger, M. Isser, S. Geis, and H. Schmidt-Böcking. *Phys. Rev. Lett*, 74:2200, 1995.

[34] V. Mergel, R. Dörner, M. Achler, Kh. Khayyat, S. Lencinas, J. Euler, O. Jagutzki, S. Nüttgens, M. Unverzagt, L. Spielberger, W. Wu, R. Ali, J. Ullrich, H. Cederquist, A. Salin, R.E. Olson, Dž. Belkić, C.L. Cocke, and H. Schmidt-Böcking. *Phys. Rev. Lett*, 79:387, 1997.

[35] R. Dörner, H. Bräuning, O. Jagutzki, V. Mergel, M. Achler, R. Moshammer, J. Feagin, A. Bräuning-Demian, L. Spielberger, J.H. McGuire, M.H. Prior, N. Berrah, J. Bozek, C.L. Cocke, and H. Schmidt-Böcking. *Phys. Rev. Lett.*, 81, 1998.

[36] R. Dörner, V. Mergel, O. Jagutzki, L. Spielberger, J. Ullrich, R. Moshammer, and H. Schmidt-Böcking. *Physics Reports*, page in print, 1999.